

Identification of Upwelling Area of the Western Territorial Waters of Indonesia from 2000 to 2017

Eko Supriyadi,^{1,2*} and Rahmat Hidayat²

¹Marine Meteorology Centre, Meteorology Climatology and Geophysical Agency (BMKG), Jakarta, Indonesia. ²Department of Geophysics and Meteorology, IPB University, Bogor, Indonesia.

Received: 2019-11-23

Accepted: 2020-03-04

Key words:

WWI;
Chl-a;
SLA;
SST;
annual cycle pattern;
upwelling.

Correspondent email:

eko.supriyadi@bmkg.go.id

Abstract The Western Waters of Indonesian (WWI) present a diverse interaction of ocean-atmosphere dynamics. One of them represents the event of Indian Ocean Dipole (IOD), El Niño–Southern Oscillation (ENSO), and upwelling. The objective of this study is to determine the dynamics of chlorophyll-a concentration (Chl-a), especially during IOD and ENSO. Also, this study is aimed to examine the temporal and spatial distribution of the upwelling area from 2000 to 2017. The data utilized consisted of Chl-a, wind stress, Sea Level Anomaly (SLA), and Sea Surface Temperature (SST). The technique used to determine the upwelling area was by examining the maximum conditions of Chl-a, the low temperature of SST, and SLA. The results showed the sea surface temperature had a relationship with the concentration of Chl-a. It was obtained if the Directional Movement Index (DMI) and N3.4 (Niño 3.4 Index) moved stably (not too fluctuation) resulting in high concentrations of Chl-a. High standard deviations of SST are recognized around the Sunda Strait (June – October). When the standard deviation of SST is high, there is also a tendency for high Chl-a concentrations, while the results of empirical calculations show that large areas of upwelling occurred in January and September respectively at 12,447.72 km² and 8,146.20 km². Based on the results of the analysis, it can be concluded that the upwelling does not only occur at the coastal area of Western Sumatra (coastal upwelling), but it also occurs in the eastern territorial waters of the Indian Ocean. In addition, the upwelling area has the same pattern as the Chl-a concentration in January - October.

©2020 by the authors. Licensee Indonesian Journal of Geography, Indonesia.
This article is an open access article distributed under the terms and conditions of the Creative Commons Attribution (CC BY NC) license <https://creativecommons.org/licenses/by-nc/4.0/>.

1. Introduction

The western territorial waters of Indonesian crossed by the equator and flanked by the Continent of Asia — Australia and The Indian and Pacific Oceans make a strong influence on the phenomenon of the monsoons, Indian Ocean Dipole (IOD) and El Niño–Southern Oscillation (ENSO). ENSO itself is a phenomenon of the relationship between air and sea occurring in the Tropical Pacific. Sometimes, the occurrence of ENSO causes extreme weather and climate affecting globally (Diaz et al., 2001; Alexander et al., 2002; Wang et al., 2017). Meanwhile, IOD is a phenomenon similar to ENSO, but it only occurs in the Tropical Indian Ocean in which the resulted impact is different. Several studies have linked that the occurrence of IOD depends on the ENSO (Baquero et al., 2002; Lau & Nath, 2003; Luo et al., 2010; Allan et al., 2011). However, some studies stated that IOD does not depend on ENSO (Saji & Yamagata, 2003; Behera et al., 2006). However, another study also revealed that IOD was affected by ENSO (Nagura & Konda, 2007; Schoot et al., 2009).

The atmospheric events mentioned above often affect the conditions of the ocean below it (Hog et al., 2016; Leber et al., 2016). One of the events is upwelling that can occur in the waters of any part of the world with specific times.

Upwelling is the event of an increase of water mass of under layers to its upper surface (Lopez-Lora et al., 2019)). This movement brings the water mass with colder temperatures, high salinity, and nutrients to the surface (Hu and Wang, 2016; Burchard et al., 2017; Cape et al., 2019).

One characteristic of this upwelling event is the increase in high Chl-a concentration (Acosta et al., 2015; Bode et al., 2017; Lehahn et al., 2017). Chl-a is the most natural phytoplankton and is the most spread throughout the world's oceans; including the classification of this type are red and green algae. An upwelling event is an excellent tool for the transfer of this Chl-a type because the maximum Chl-a value is not always close to the water surface but sometimes below the euphotic zone. The euphotic layer is a layer of depth with light intensity still allowing for photosynthesis. The limit of the depth of the euphotic zone is more or less to the depth where the light intensity remains 1% of the intensity of sunlight falling on the surface. This depth is the preferred location of Chl-a because the rate of photosynthesis is balanced with the rate of its respiration (Nontji, 2008).

Besides, the upwelling event is also related to the dynamics of the SST local waters (Napitu et al., 2015; Chen et al.,

2015; Varela et al., 2016). The dynamic of SST in the Indian Ocean is directly related to the event of IOD; although it does not rule out the effect of ENSO from the Pacific Ocean, it could affect the physical upwelling process in the Indian Ocean (Chen et al., 2015). The factor of the wind also affects the upwelling event. Research conducted by Chen et al. (2015) discovered a relationship between local wind changes and upwelling variability. Furthermore, the wind moving will bring up the pressure on the water surface called wind stress. Wind stress is calculated as the relationship between wind speed and the density of air above the ocean. This wind stress retains a relation to the transport of Ekman, which later will affect the direction of motion of the upwelling process itself (Spall & Pedlosky, 2013; Wieners et al., 2016).

Several studies have been carried out to determine the upwelling occurrence in the waters of Indonesian such as that conducted by Susanto et al. (2001) that studied the evolution of upwelling along the waters of Southern Java to Western Sumatra. It was explained that upwelling in this location occurred during the southeast monsoons around May to October. Especially during the El Niño year, upwelling reaches the waters of Western Sumatra in November. In the year of the El Niño type, the upwelling intensity is stronger than the La Niña type. Another research conducted by Kunarso et al. (2011) examined the upwelling on the southern coast of Java to Timor during the southeast monsoons. At the time of the upwelling event, the Chl-a value reached a maximum in August and the lowest SPL value in June. Ogata et al. (2017) added that the average of vertical upwelling velocity in the Indian Ocean reaches a maximum value below the thermocline layer.

Further, based on the several parameters above, those have supported to find out the location of the upwelling area, because almost all the requirements for upwelling have been fulfilled. Our hypothesis suggests that the conditions for upwelling occurrence are when the Chl-a concentration is high, the SST is low, and the wind stress is high. Therefore, this study aims at the identification of upwelling followed by dynamics of parameters during IOD/ENSO, identifying the extent of upwelling areas in the WWI and their relationship to Chl-a, SST, and SLA.

2. The Methods

The research site is the WWI at coordinates $90,52^{\circ}$ — $105,73^{\circ}$ east longitude, $10,06^{\circ}$ north latitude — $8,27^{\circ}$ south latitude (Fig. 1). There are four types of data used in this study. First, Chl-a data were obtained from Aqua MODIS satellites from 2001 to 2017. This data can be downloaded at <http://www.oceancolor.gfsc.nasa.gov> in the format of 3 netCDF of Level-3 Standard Mapped Image (SMI) (the data have been corrected in the form of local topography). Second, wind stress data were obtained through the METOP satellite producing data called ASCAT (The Advanced Scatterometer); the time range of data used was from 2009 to 2017. These data can be downloaded at <http://coastwatch.pfeg.noaa.gov>. Third, SLA data were obtained from the European Maritime Monitoring Center

(Copernicus) from 2009 to 2017. The data can be downloaded at <http://marine.copernicus.eu/services-portfolio/access-to-products/>; it can be downloaded by registering yourself first. Ultimately, the fourth data utilized were SST data series to conduct a study on IOD/ENSO. This data was obtained in the Hadley Meteorological Center, England, at <https://www.metoffice.gov.uk/hadobs/hadisst/data/download.html>. The time range of data used was from 2000 to 2017.

To obtain the distribution of Chl-a in the research area, chlorophyll data from Aqua Modis satellite is processed according to each month so that it is obtained seasonal cycle pattern. Considering the small value of chlorophyll, the processing is calculated logarithmically for the value of the chlorophyll. The identical thing is performed for wind stress and SLA data only without implementing logarithmical calculation.

Furthermore, to determine the effect of sea surface temperature on the IOD/ENSO response, the sea surface temperature data that have been obtained are made its SST index values through standardization, namely:

$$SST_{index} = \frac{SST_t - SST_{std}}{SST_{std}} \quad (1)$$

with the definition of BMKG (2010), the conditions for the occurrence of IOD and ENSO are:

IOD is with the value of $SST_{max} \geq 0.4$ or $SST_{min} \leq -0.4$

ENSO is weak with the value of $\pm 0.5 \leq SST_{index} < \pm 1$

ENSO is moderate with the value of $\pm 1 \leq SST_{index} < \pm 2$

ENSO is strong with the value of $SST_{index} \geq 2$ or $SST_{index} \leq -2$

Equation 1 is then plotted in time series, and the upper and lower limit values of the categories mentioned above are applied to determine the IOD and ENSO indexes at each time to be observed.

Then, we have a time series profile for Chl-a and SST in the form of IOD or ENSO. Due to the fluctuations of Chl-a is affected by SST, especially in tropical waters (Nurdin et al.,

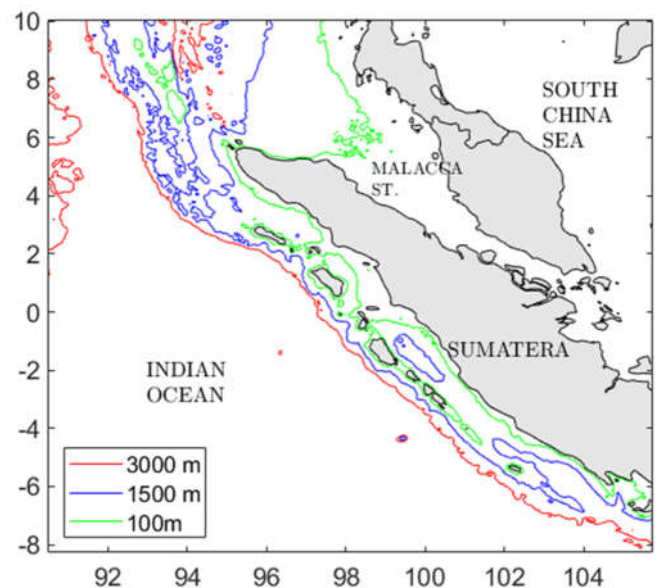


Figure 1. Upwelling research site. The color line shows bathymetry. The data source is taken from ETOPO 1 dataset.

2013; Kumar et al., 2016). The next step is to calculate the IOD difference against ENSO to find its relation to Chl-a. The result is described in the following subsection.

From the spatial maps and graphs having been obtained, an analysis is carried out to identify the upwelling area in WWI. The basis of empirical calculations identification of this upwelling area is based on three parameters; those are Chl-a concentration, standard deviation of SST, and SLA. The Chl-a concentration taken is in the range of values from one to the maximum value; the SST value is in the range of its minimum values up to its average value, and the SLA values are from its minimum value up to 0.1 m. The three parameters were previously equated with the first spatial resolution following one of the highest parameter resolutions; then a logical sequence index was made to be then overlapped one another so that the upwelling region was known.

The determination of the upwelling area is based on the explanation of Susanto et al. (2001) explaining the upwelling conditions can occur when Chl-a is high, SST is cold, and SLA is low. The next step is to determine the area of the upwelling area after identifying the location of the upwelling.

3.Result and Discussion

The Dynamics of Chl-a at IOD/ENSO

The results of data processing showed that the Malacca Strait has a relatively high concentration of Chl-a throughout the year. However, these results were diverse from what happened on the western coast of Sumatra (Fig. 2). By July, Chl-a developed to appear around the Sunda Strait and reached its peak in September, then it decreased in October.

The high Chl-a in the Malacca Strait (marked with light color in Fig.2) is caused by the exchange of river water from Malaysia such as Pulau, Redan, Karang, Permas, Perak, Rambah, Pontian Kechil, Pontian Besar, Ayer Baloi, Sanglang, Benut, Batu Pahat, and Kedah River. It was added with some rivers from Sumatra like Kampar and Asahan, Siak, Indragiri, and Batanghari river. The water stream of these rivers provides nutrients for Chl-a in the Malacca Strait. Similar results were also reported by Siswanto and Tanaka (2014) who examined the river discharge with Chl-a in Malacca Strait.

Some other calculations were also obtained in this study included the rate and the trend of concentration. Every month in 1 year, the rate of Chl-a value decreased by 0.0034 mg.m⁻³. However, during the observation period of 180 months (2002 - 2017) shows the monthly value (seasonal) of Chl-a with a fixed trend of 7.10⁻⁵ mg.m⁻³. Simultaneously, if the calculation is added by removing the value of the trend, there can still be a continuing trend of 2.10⁻⁵ mg.m⁻³. It means that the concentration of Chl-a at the WWI has remained stable over the study period.

The distribution annual cycle of Chl-a in the WWI is presented in Fig. 3. It was noted that the concentration reached 30 mg.m⁻³ in 2011. Because the Chl-a value fluctuates throughout the year, it is not enough if it merely displays the distribution of values in a time series sequence.

The further step is to collect Chl-a values in the same

year to be compared in subsequent years, as presented in Fig. 3. The spatial distribution of Chl-a in western Indonesia is concentrated at 100° and 104° east longitude. This is related to the exchange of river water in the Malacca Strait (Siswanto and Tanaka, 2004). Meanwhile, when reviewed temporally, it was noted in the middle of 2006, 2008, 2010, 2011, 2013, and 2016 that Chl-a concentration showed high values up to 1.4 mg.m⁻³. Especially for the 2011 year, it is seen that Chl-a concentration has a strong effect up to 103° east longitude.

Generally, Chl-a develops following the changes of its surrounding ocean temperature. High Chl-a concentration is at low ocean temperatures. However, the highest concentration does not follow the lowest ocean temperatures (Kunarso et al., 2011). It is as if Chl-a is developing at a specific optimum temperature range. For this reason, SST conditions on the concentration of Chl-a will be reviewed using

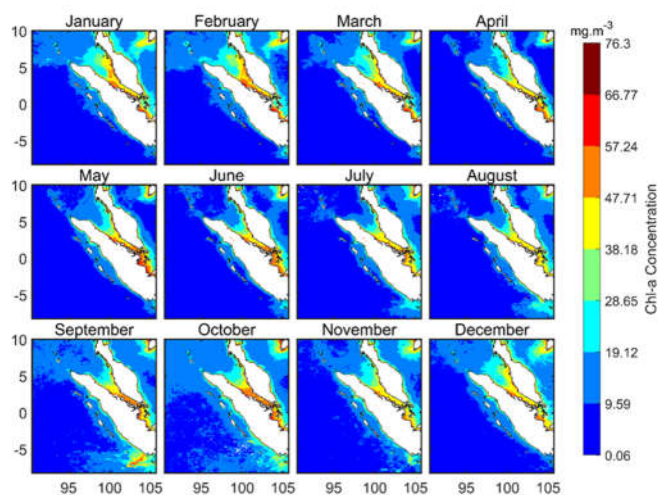


Figure 2. Distribution annual cycle of Chl-a at the WWI based on Modis Aqua satellite (2002 - 2017). The data displayed is composite 1 month for 1 year. The maximum and minimum values on the color bar correspond to the maximum and minimum concentrations of Chl-a.

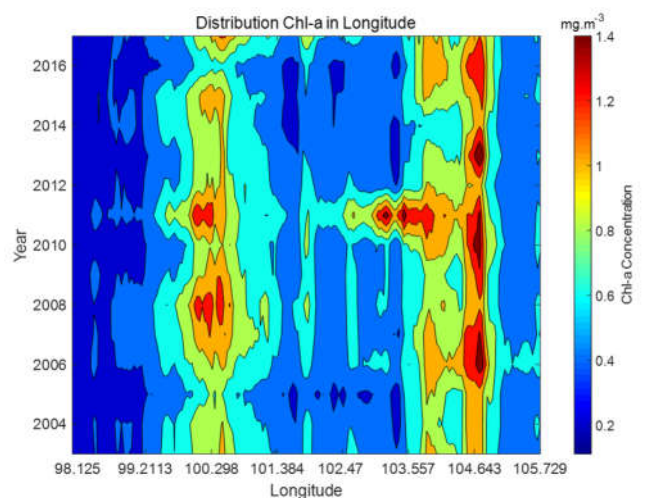


Figure 3. Time series of Chl-a concentration in the WWI. The value of Chl-a concentration is calculated annually to find out what year the maximum concentration is. The red vertical line represents the year with the maximum Chl-a concentration (~1.4 mg.m⁻³).

the value of DMI for IOD. In addition, considering that the Waters of Indonesian were also affected by the ENSO system of the Pacific Ocean. The N3.4 (Niño 3.4 Index) was also included to find out how much the impact of the Western Pacific temperature anomaly on the Chl-a concentration (Fig. 4).

Figure 4a shows the value of DMI and N3.4 (Niño 3.4 Index) in the research site. IOD value $\geq 0.4^{\circ}\text{C}$ ($\leq -0.4^{\circ}\text{C}$) refers to Sea Surface Temperature $>0.5^{\circ}\text{C}$ warmer ($<-0.5^{\circ}\text{C}$ cooler) (BMKG, 2010). Positive DMI was seen to take place in mid-2002, mid-2006, 2012, 2015, and mid-2016. Meantime, negative DMI took place in 2004, 2005, mid-2010, 2013, 2014, and 2016. Furthermore, the N3.4 (Niño 3.4 Index) (El niño) with the average category emerged in 2003, 2007, mid-2009, and mid-2015. As for the N3.4 (Niño 3.4 Index) (La Nina), the average category emerged in mid-2007, mid-2010, mid-2011, and mid-2016.

When Fig. 4a is connected to Fig. 3, it is discovered that the temperature difference in the Indian Ocean (IOD) and Pacific Ocean (N3.4/Niño 3.4 Index) which is not too fluctuation results in high Chl-a concentrations. It is indicated by the vertical red line in Fig. 3. It is required for further study to explain the event. Furthermore, to see how much effect of the IOD and N3.4 (Niño 3.4 Index) on the chlorophyll index is calculated through the coefficient of determination. The results are 0.56 (Fig. 4b). It shows there is a dominant relationship between Chl-a concentration and the changes of ocean temperature (Indian-Pacific), especially WWI. Notice that the index has been standardized to omit

the influence of the mean and standard deviation of the original data (Johnson and Bhattacharyya, 2010).

To simplify the analysis of the distribution of Chl-a to SST, the standard deviation values were calculated (Fig. 5). It was marked from June to October that the high standard deviation values of SST were detected around the Sunda Strait and then reappeared in March. Whereas, on the Western coast of Sumatra, the standard deviation of SST obtained was relatively low. When the SST standard deviation was high, there was a tendency for high Chl-a concentrations (July-October, see Fig. 2). The high standard deviation of SST in the Sunda Strait occurs during the east monsoons. The high standard deviation of SST is associated with the low standard deviation of SST, and this is in line with the results of research conducted by Susanto and Marra (2005), and Kunarso et al. (2011).

Upwelling from parameters of SST, wind stress, and SLA

To identify the upwelling event in WWI, it is then connected with physical parameters like the standard deviation of SST (Fig. 5), wind stress (Fig. 6), SLA (Fig. 7). The results of data processing showed that the average SST was colder with a value of 27°C starting to form around $5^{\circ} - 8^{\circ}$ east latitude, starting from April to November. The Malacca Strait tends to be warm all year round, the South China Sea (SCS) is relatively cold from November to March. However, it can be noted in the standard deviation values (Fig. 5), the higher (lower) the standard deviation of SST, the lower (higher) the SST produced.

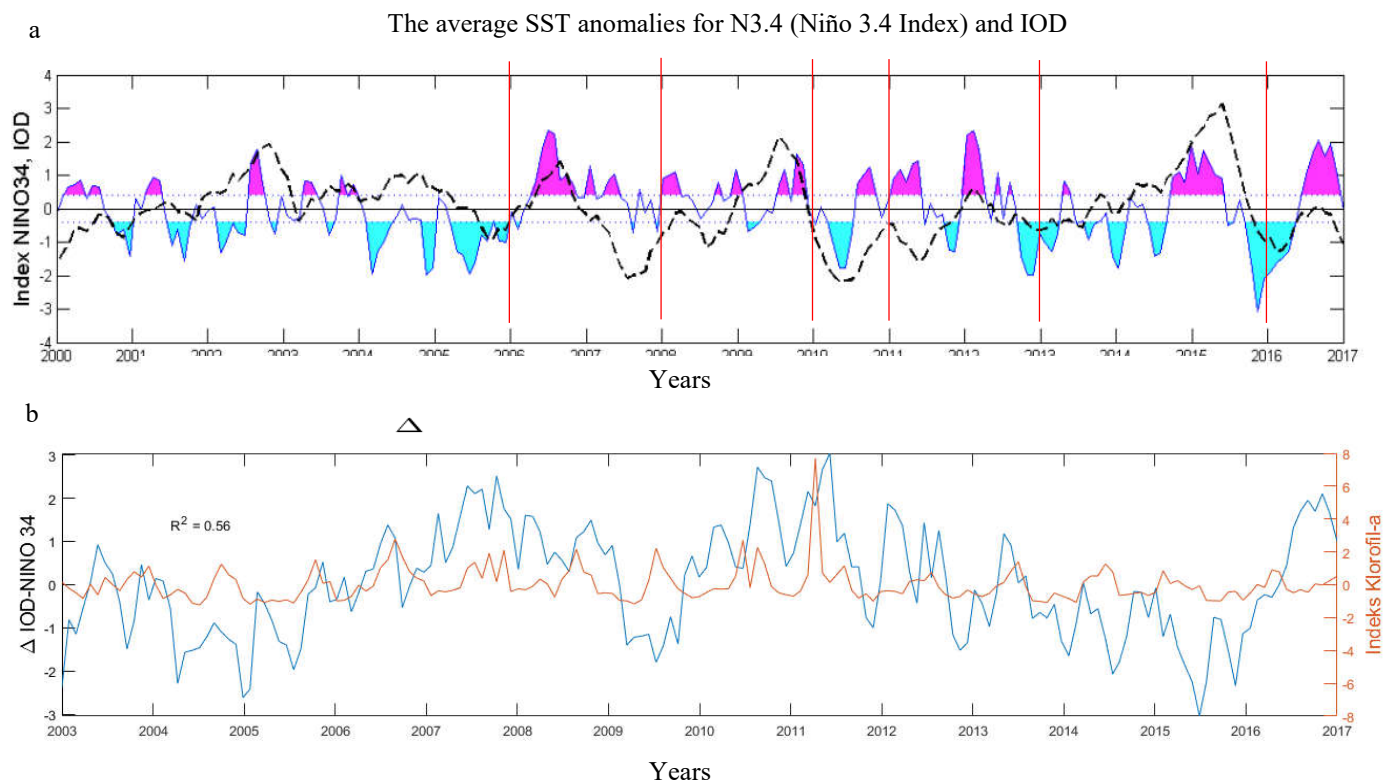


Figure 4.(a) Average of SST anomalies for N3.4 (Niño 3.4 Index) (dashed black lines) and DMI (colored areas) during the period 2000 - 2017 (monthly effect and trends have been removed). The magenta plot shows the DMI value $\geq 0.4^{\circ}\text{C}$, while the cyan color states the DMI value $\leq -0.4^{\circ}\text{C}$. The red vertical line represents the year in which the Chl-a reached its peak (see Fig. 3). (b) Relationship between the difference in the value of IOD with N3.4 (Niño 3.4 Index) (blue line) to the Chl-a index (brown line) from 2003 to 2017.

Moreover, the SST in the Malacca Strait is warmer than the temperature of the Western Waters of Sumatra (WWS) as shown in Fig. 5. Kumalawati (2004) reported that the waters with warm temperatures and low salinity make the area rich in Chl-a. The high Chl-a occurred in the Malacca Strait was also confirmed by Siswanto and Tanaka (2014), especially during the northeast monsoons. We suspect the waters around the SCS have a high content of Chl-a because many streams flowing there. It added with the SCS Sea position around the equator can make SST around warmer.

Unlike the Malacca Strait, the WWS has relatively little distribution of Chl-a. It can be comprehended because there are very few rivers flowing to the WWS, and it is added by relatively low SST compared to Malacca Strait (Fig. 5). In September, the maximum concentration of Chl-a is 37 mg.m⁻³ around the Sunda Strait (Western area of Sumatra).

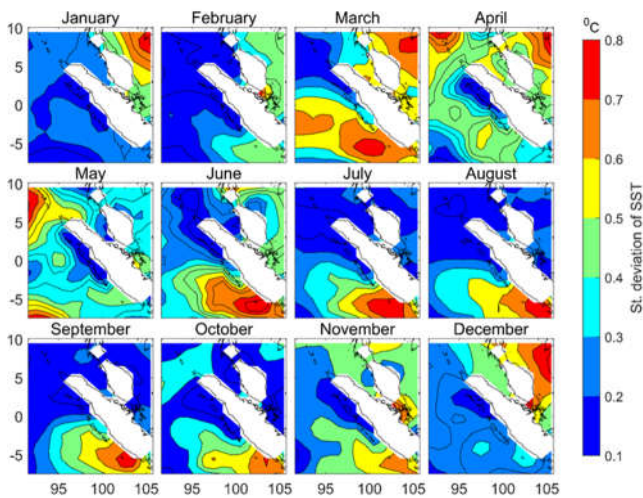


Figure 7. The annual cycle of SLA is a result of wind stress events in WWI for the period 1993 - 2017. The inter-contour interval is 0.02 m. A thick black line represents the parallel Sea Level of 0 m, a thin black line of >0 m, and a dashed black line of <0 m.

Then, the distribution of Chl-a go forward to the southwest crossing the Indonesian Exclusive Economic Zone (EEZ) for 200 miles.

Furthermore, based on the value of SLA in the WWS (Figure. 7), an anomaly with value <0 m occurred from February to March. Subsequently, it disappeared and was replaced by a positive SLA value from April to July. Then, the negative SLA value re-occurred in the Sunda Strait from August to September. Unlike with the case of the WWS, the incidence of low and high SLA appears with a matching pattern (>0 m from October to March and <0 m from April to September) in the waters of SCS.

The event of SLA is related to wind stress as a result of east monsoons occurring from May to October. Wind stress during the east monsoons causes low wind stress curl in West Sumatra, in contrast to it, there is a high wind stress curl from November to April during the west monsoons (Fig. 6). The wind stress curl was causing the Ekman pumping in waters experiencing high wind speeds. The result cre-

ates an “space” in the water column and marked by a negative contour in Fig. 7.

The extent of the upwelling area

Based on the explanation above, a classification table can then be made to determine the occurrence time of upwelling. The requirements for the occurrence of upwelling areas have previously been explained in the methodology section. Seen in Table 1, August and September meet the criteria for upwelling. However, the distribution is only limited to an estimation. Empirical evidence of calculations regarding the time and the place of the upwelling occurrence is presented in Fig. 8. It is noteworthy that the results obtained were averaged from 2000 to 2017.

When viewed temporally, the upwelling occurs evenly in all months not only in areas with high Chl-a concentrations. Seen in April-July, upwelling was not detected in WWI. It is because the calculations include the influence of SST and SLA. Total areas of the occurrence of upwelling in January and September, respectively, are 12447.72 km² and 8146.20 km² (Table 1). From the results obtained, it turns out that the upwelling does not only occur in the coastal area (i.e., coastal upwelling), but it also can occur in the open sea.

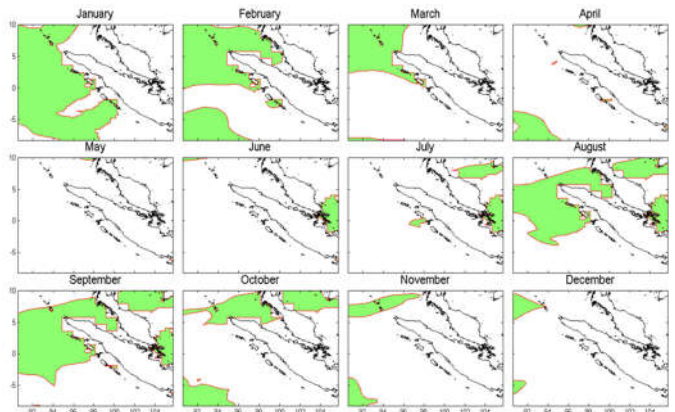


Figure 8. Upwelling areas (predicted) each month (from 2000 to 2017) marked by green contours.

After identifying the location of this upwelling, there is a fundamental question which is why does the Malacca Strait have greater Chl-a concentration than the western coast of Sumatra, not experience upwelling events? While the south coast of Java having a smaller Chl-a concentration undergoes a more massive upwelling process (Susanto et al., 2001). It can be comprehended because of the Southern Waters of Malacca experiences shallower bathymetry than the South coast of Java (Fig. 1). Deep bathymetry is needed as an effective heat transfer process for the upper and lower seawater columns. It should be considered that the position of the South coast of Java is directly related to the open Indian Ocean where, in the southeast monsoons (July – September), the wind blows towards the coast of Sumatra until it is deflected to the equator. Thus, the wind stress produced is of high value and results in a deficit of the seawater column along the South coast of Java. However, it needs to be considered that the wind stress factor is still one of the determi-

Table 1. The total area of upwelling, according to Fig. 7 ($\times 10^3 \text{ km}^2$)

	Jan.	Feb.	Mar.	Apr.	May	Jun.	Jul.	Aug.	Sept.	Oct.	Nov.	Dec.
Total Area	12.4	7.33	4.51	1.54	0.05	0.83	0.84	6.62	8.15	2.45	1.34	0.72

nations of the upwelling area in addition to a combination of the effect of the content Chl-a and SST. Therefore the Ekman spiral often referred to as an upwelling generator does not affect the conditions of the two bathymetries of the place (i.e., Malacca and Sunda Strait). It is because the Ekman effect stops at a depth of 120 m (Lenn and Chereskin, 2009). Therefore, what becomes most causes of upwelling in the WWI are SST, wind stress, and SLA.

Furthermore, Yuliana and Mutmainnah (2018) reported physical parameters as the turbidity derived from the river deposition has a positive correlation with Chl-a. While Gitelson (2007) have found wavelengths, 667 and 748 nm from MODIS satellite allows estimate the Chl-a with it RMSE 11 mg/m^3 . That values are better than the 678 and 748 nm wavelengths that result in the RMSE below 12.7 mg/m^3 . Those results also supported this research that the turbidity caused by the rivers flow on WWI can be used as a reference to determine the concentration of Chl-a.

Conclusion

Even though Malacca Strait has a narrower waters area than the Western coast of Sumatra, the produced Chl-a is relatively higher than other areas. The phenomenon may be due to many of rivers stream flowing to the estuary, and it provides nutrients for Chl-a add with the SST relatively warmer factor because of close to the equator. Chl-a in the western area of Indonesia is generally concentrated at coordinates 100° and 104° east longitude. When viewed temporally, the Chl-a concentration had a maximum value in 2006, 2008, 2011, 2013, and 2016 with an amount of 1.4 mg.m^{-3} .

The SST has a relationship to the Chl-a concentration. It is obtained if the DMI and N3.4 (Niño 3.4 Index) move stably (not too fluctuation) resulting in high Chl-a concentration. The high standard deviation of SST is recognized around the Sunda Strait (from June to October). When the standard deviation of SST is high, there is a tendency for high Chl-a concentration as well. In addition, the month coincides with the east monsoons. In the same month, the WWI had a low standard deviation of SST.

From the calculation results, it was obtained the high intensity of upwelling occurred in January and September for the observation range of 2000 to 2017. Upwelling areas occur evenly on the west coast of Sumatra with an area of 12447.72 km^2 and 8146.20 km^2 . The area of high upwelling occurred is affected when the Chl-a concentration is high, SST is cold, and SLA is low. It should be noted although WWI has a high of Chl-a concentration and the two factors (i.e. SST and SLA) do not support, the upwelling unable to dominate. So, it is important to look at these factors overall.

Acknowledgments

This research did not receive funding assistance from external parties. In addition, the authors also want to express their appreciation to the blind reviewers who have provided input for improvement in this manuscript.

References

- Alexander, M. A., Bladé, I., Newman, M., Lanzante, J.R., Lau, N.-C., & Scott, J. D. (2002). The Atmospheric Bridge: The Influence of ENSO Teleconnections on Air-Sea Interaction over the Global Oceans. *Journal of Climate*, 15(16), 2205–2231.
- Allan, R., Chambers, D., Drosowsky, W., Hendon, H., Latif, M., Nicholls, N., Smith, I., Stone, R.G., Tourre, Y. (2001). Is there an Indian Ocean Dipole and is it Independent of the El Niño-Southern Oscillation?. *CLIVAR Exchanges*, 6(3), 18-22.
- Acosta, A.C., Morales, C. E, Hormazabal, S., Andrade, I., & Ramirez, M. A. C. (2015). Phytoplankton Phenology in the Coastal Upwelling Region off Central-Southern Chile (35°S – 38°S): Time-space Variability, Coupling to Environmental Factors, and Sources of Uncertainty in the Estimates. *Journal of Geophysical Research: Oceans*, 120(2), 813–831.
- Baquero-Bernal, A., Latif, M., & Legutke, S. (2002). On Dipolelike Variability of Sea Surface Temperature in the Tropical Indian Ocean. *Journal of Climate*, 15(11), 1358–1368.
- Behera, S. K., Luo, J. J., Masson, S., Rao, S. A., Sakuma, H., & Yamagata, T. (2006). A CGCM Study on the Interaction between IOD and ENSO. *Journal of Climate*, 19(9), 1688–1705.
- BMKG. (2010). Press Release "Kondisi Cuaca Ekstrem dan Iklim Tahun 2010 - 2011".
- Bode, A., Varela, M., Prego, R., Rozada, F., & Santos, M. D. (2017). The Relative Effects of Upwelling and River Flow on The Phytoplankton Diversity Patterns in the Ria of a Coruña (NW Spain). *Marine Biology*, 164(4), 93.
- Burchard, H., Basdurak N. B., Grawe, U., Knoll, M., Mohrholz, V., & Muller S. (2017). Salinity inversions in the thermocline under upwelling favourable winds. *Geophysical Research Letters*, 44(3), 1422-1428.
- Cape, M. R., Straneo, F., Beaird N., Bundy R. M., & Charette M. A. (2019). Nutrient release to oceans from buoyancy-driven upwelling at Greenland tidewater glaciers. *Nature Geoscience*, 12, 34-39.
- Chen, G., Han, W., Li, Y., & Wang, D. (2015). Interannual Variability of Equatorial Eastern Indian Ocean Upwelling: Local versus Remote Forcing. *Journal of Physical Oceanography*, 46(3), 789–807.
- Diaz, H. F., Hoeling, M.O., & Eischeid, J. K. (2001). ENSO Variability, Teleconnections and Climate Change. *International Journal of Climatology*, 21(15), 1845–1862.
- Gitelson, A. A., Schalles, J. F., & Hladik C. M. (2007). Remote chlorophyll-a retrieval in turbid, productive estuaries: Chesapeake Bay case study. *Remote Sensing of Environment*, 109, 464-472.
- Hogg, A. M., Spence, P., Saenko, O. A., & Downes, S. M. (2016). The Energetics of Southern Ocean Upwelling. *Journal of Physical Oceanography*, 47(1), 135–153.
- Hu, J., & Wang X.H. (2016). Progress on Upwelling studies in the China seas. *Reviews of Geophysics*, 54(3), 653-673.
- Johnson, R. A, Bhattacharyya G. K. (2010). Statistics Principles and

Methods. Sixth edition, John Willey and Sons, USA.

- Kumalawati, A. S. (2004). *Variabilitas parameter oseanografi dan sebaran klorofil-a di Perairan Nangroe Aceh Darussalam pada Bulan Oktober-November*. Institut Pertanian Bogor.
- Kumar, G. S., Prakash, S., Ravichandran M., Narayana, A. C. (2016). Trends and relationship between chlorophyll-a and sea surface temperature in the central equatorial Indian Ocean. *Remote Sens. Lett.* 7(11):1093–1101.
- Kunarso, K., Hadi, S., Ningsih, N. S., & Baskoro, M. S. (2011). Variabilitas Suhu dan Klorofil-a di Daerah Upwelling pada Variasi Kejadian ENSO dan IOD di Perairan Selatan Jawa sampai Timor. *ILMU KELAUTAN: Indonesian Journal of Marine Sciences*, 16(3), 171-180.
- Lau, N.-C., & Nath, M. J. (2003). Atmosphere–Ocean Variations in the Indo-Pacific Sector during ENSO Episodes. *Journal of Climate*, 16(1), 3–20.
- Leber, G. M., Beal, L. M., & Elipot, S. (2016). Wind and Current Forcing Combine to Drive Strong Upwelling in the Agulhas Current. *Journal of Physical Oceanography*, 47(1), 123–134.
- Lehahn, Y., Koren, I., Sharoni, S., d'Ovidio, F., Vardi, A., & Boss, E. (2017). Dispersion/Dilution Enhances Phytoplankton Blooms in Low-Nutrient Waters. *Nature Communications*, 8, 14868.
- Lenn, Y.-D., & Chereskin, T. K. (2009). Observations of Ekman Currents in the Southern Ocean. *Journal of Physical Oceanography*, 39(3), 768–779.
- Lopez-Lora, M., Chamizo, E., Rozmaric, M., & Louw, D. C. (2019). Presence of ²³⁶U and ²³⁷Np in a marine ecosystem: The Northern Benguela Upwelling System, a case study. *Science of the Total Environment*. 708, 135222.
- Luo, J.-J., Zhang, R., Behera, S. K., Masumoto, Y., Jin, F.-F., Lukas, R., & Yamagata, T. (2010). Interaction between El Niño and Extreme Indian Ocean Dipole. *Journal of Climate*, 23(3), 726–742.
- Nagura, M., & Konda, M. (2007). The Seasonal Development of an SST Anomaly in the Indian Ocean and Its Relationship to ENSO. *Journal of Climate*, 20(1), 38–52.
- Napitu, A. M., Gordon, A. L., & Pujiana, K. (2015). Intraseasonal Sea Surface Temperature Variability Across the Indonesian Seas. *Journal of Climate*, 28(22), 8710–8727.
- Nurdin, S., Mustapha M. A., & Lihan T. (2013). The relationship between sea surface temperature and chlorophyll-a concentration in fisheries aggregation area in the archipelagic waters of spermonde using satellite images. *AIP Conf. Proc.* 1571(1):466–472.
- Nontji, A. (2008). *Plankton Laut*. Jakarta: Yayasan Obor Indonesia Publisher.
- Ogata, T., Nagura, M., & Masumoto, Y. (2017). Mean Subsurface Upwelling Induced by Intraseasonal Variability over the Equatorial Indian Ocean. *Journal of Physical Oceanography*, 47(6), 1347–1365.
- Saji, N. H., & Yamagata, T. (2003). Possible impacts of Indian Ocean Dipole Mode Events on Global Climate. *Climate Research*, 25(2), 151–169.
- Schoot, F. A., Xie, S. P. & McCreary, J. P. (2009). Indian Ocean Circulation and Climate Variability. *Reviews of Geophysics*, 47(1), 1-47.
- Siswanto, E. & Tanaka, K. (2014). Phytoplankton Biomass Dynamics in the Strait of Malacca within the Period of the SeaWiFS Full Mission: Seasonal Cycles, Interannual Variations and Decadal-Scale Trends. *Remote Sensing*, 6 (4), 2718-2742.
- Spall, M. A., & Pedlosky, J. (2013). Interaction of Ekman Layers and Islands. *Journal of Physical Oceanography*, 43(5), 1028–1041.
- Susanto, R. D., Gordon, A. L., & Zheng, Q. (2001). Upwelling along the Coasts of Java and Sumatra and its Relation to ENSO. *Geophysical Research Letters*, 28(8), 1599–1602.
- Susanto, R. D., & Marra, J. (2005). *Chlorophyll a Variability Along the Southern Coasts of Java and Sumatra*. *Oceanography*, 18 (4), 124-127.
- Varela, R., Santos, F., Gómez-Gesteira, M., Álvarez, I., Costoya, X., & Días, J. M. (2016). Influence of Coastal Upwelling on SST Trends Along the South Coast of Java. *PLoS ONE*, 11(9).
- Wang, C., Deser, C., Yu, J.-Y., DiNezio, P., & Clement, A. (2017). El Niño and southern oscillation (ENSO): a review. In *Coral Reefs of the Eastern Tropical Pacific* (pp. 85–106). Springer.
- Wieners, C. E., Dijkstra, H. A., & de Ruijter, W. P. M. (2016). The Influence of the Indian Ocean on ENSO Stability and Flavor. *Journal of Climate*, 30(7), 2601–2620.
- Yuliana & Mutmainnah. (2017). Kandungan klorofil-a dalam kaitannya dengan parameter fisika-kimia perairan di Teluk Jakarta, 1(2), 206-213.